Published online 8 September 2011 *Nucleic Acids Research, 2012, Vol. 40, No. 1* ***159–169***
doi:10.1093/nar/gkr723

Histone hypoacetylation is required to maintain late replication timing of constitutive heterochromatin

Corella S. Casas-Delucchi[1,2], Joke G. van Bemmel[2], Sebastian Haase[2], Henry D. Herce[1], Danny Nowak[2], Daniela Meilinger[3], Jeffrey H. Stear[2], Heinrich Leonhardt[3] and M. Cristina Cardoso[1,2,*]

[1]Department of Biology, Technische Universität Darmstadt, 64287 Darmstadt, [2]Max Delbrück Center for Molecular Medicine, 13125 Berlin and [3]Department of Biology II, Center for Integrated Protein Science, Ludwig Maximilians University Munich, 82152 Planegg-Martinsried, Germany

Received March 1, 2011; Revised and Accepted August 22, 2011

ABSTRACT

The replication of the genome is a spatio-temporally highly organized process. Yet, its flexibility throughout development suggests that this process is not genetically regulated. However, the mechanisms and chromatin modifications controlling replication timing are still unclear. We made use of the prominent structure and defined heterochromatic landscape of pericentric regions as an example of late replicating constitutive heterochromatin. We manipulated the major chromatin markers of these regions, namely histone acetylation, DNA and histone methylation, as well as chromatin condensation and determined the effects of these altered chromatin states on replication timing. Here, we show that manipulation of DNA and histone methylation as well as acetylation levels caused large-scale heterochromatin decondensation. Histone demethylation and the concomitant decondensation, however, did not affect replication timing. In contrast, immuno-FISH and time-lapse analyses showed that lowering DNA methylation, as well as increasing histone acetylation, advanced the onset of heterochromatin replication. While *dnmt1*$^{-/-}$ cells showed increased histone acetylation at chromocenters, histone hyperacetylation did not induce DNA demethylation. Hence, we propose that histone hypoacetylation is required to maintain normal heterochromatin duplication dynamics. We speculate that a high histone acetylation level might increase the firing efficiency of origins and, concomitantly, advances the replication timing of distinct genomic regions.

INTRODUCTION

The duplication of the genome prior to cell division occurs in a spatially and temporally organized manner (1). Studies describing DNA replication on a cytological level have demonstrated that sites of DNA synthesis are detectable as discrete nuclear foci, each corresponding to a cluster of several simultaneously active replication forks (2). On a spatial level, the number and location of these foci change as the cell progresses through S-phase, resulting in distinct nuclear patterns associated with early, mid, and late replicating regions (3–6). The temporal order of replication reflects the higher order organization of the genome. During the first half of S-phase, euchromatic regions are replicated followed by facultative heterochromatin during mid S-phase and finally constitutive heterochromatic regions in the second half of S-phase (7,8).

The control of this spatial and temporal organization is intrinsically related to the coordinated firing of replication origins at distinct chromatin regions (9). Understanding the nature of this regulation has been complicated by the fact that a consensus sequence for replication origins has not been identified in higher eukaryotes (10), hampering the studying of replication origin firing dynamics. Moreover, certain regions change their replication timing during development or according to gene activity (11–13). This observed plasticity has led to the suggestion that replication timing is not sequence driven, but rather modulated by dynamic changes in chromatin structure and composition (14). Modifications of DNA and histones

*To whom correspondence should be addressed. Email: cardoso@bio.tu-darmstadt.de
Present addresses:
Joke G. van Bemmel, Division of Gene Regulation, Netherlands Cancer Institute, 1066 CX Amsterdam, The Netherlands.
Sebastian Haase, Department of Experimental Physics, Freie Universität of Berlin, 14195 Berlin, Germany.
Jeffrey H. Stear, Institut für Biologie, Humboldt Universität zu Berlin, 10115 Berlin, Germany.

have been demonstrated to play a central role in defining chromatin structure on a local level, making them ideal candidates for regulators of replication timing (15).

Several lines of evidence support the idea that replication timing is regulated by chromatin structure. Specific chromatin modifications are known to correlate with replication timing, such as histone acetylation with early replication in *Drosophila* (16). For example, changes from early to late replication are accompanied by repackaging of DNA into nucleosomes containing deacetylated histones (17). In contrast, other chromatin markers, including DNA and H3K9 (tri)methylation (H3K9m3), are associated with late replication at particular loci (18). Disrupting the normal pattern of chromatin modifications within the nucleus has been associated with changes in replication timing. For instance, inhibition of histone deacetylases (HDACs) by treatment with trichostatin A (TSA) leads to earlier replication of the β-globin locus (19). In yeast, deleting the histone deacetylase Rpd3 results in earlier replication of late origins (20). Interestingly, knocking down HP1 in *Drosophila* Kc cells results in delayed replication of euchromatic repeats and advanced replication of centromeric heterochromatin (21). Altogether, these data indicate a connection between the epistate of chromatin and its replication timing. However, the exact nature of this relationship, especially in mammals, remains unclear.

To address how chromatin modifications influence replication timing, we focused on the replication of constitutive heterochromatin (22). Constitutive heterochromatin exhibits a complex chromatin landscape, marked by high levels of DNA methylation, H3K9m3 and histone hypoacetylation. These modifications help define a highly condensed nature, and in mouse cells these regions assemble into higher order aggregates known as chromocenters (23). These structures are composed of $\sim 10^5$ major satellite DNA repeats (24) and can be visualized by DNA staining with DAPI as round, highly condensed structures. Due to their prominent structure, chromocenters represent an identifiable landmark within the nucleus that can be easily visualized throughout the cell cycle. It is thus possible to directly image the interactions of the replication machinery with the chromocenters during S-phase.

We have undertaken a comprehensive study investigating the role of chromatin markers in defining the late replication timing of constitutive heterochromatin. The late replication timing of chromocenters was assessed by quantification of replication patterns and colocalization of early replication foci with chromocenters by immuno-FISH. We also performed live cell imaging using fluorescently tagged proteins to label the replication machinery and major satellite repeats and followed chromocenter replication in real time. We manipulated the epistate of constitutive heterochromatin by altering all three of its chromatin hallmarks: histone hypoacetylation, accumulation of H3K9m3 and DNA methylation. These manipulations allowed us to identify several conditions in which constitutive heterochromatin underwent hyperacetylation. This increase was associated with an earlier onset of replication. We therefore conclude that hypoacetylation, but not DNA methylation or accumulation of H3K9m3, plays a critical role in defining late-replicating regions of the genome. Our results put into context observations from different model systems, as well as from *in situ* and *in vitro* experiments and demonstrate that histone hypoacetylation is an indispensable mechanism determining late replication timing.

MATERIALS AND METHODS

Cells

Wild-type mouse fibroblasts, *suv39h1/2* double null, $p53^{-/-}$ null as well as $p53^{-/-}$ and $dnmt1^{-/-}$ double knockout cells (MEF-WT, MEF-D15, MEF-P, MEF-PM, respectively) were grown as previously described (25,26). Cells used for immunofluorescence analysis were grown on glass coverslips. TSA (Sigma-Aldrich, Steinheim, Germany) treatment was performed with a final concentration of 20 nM over 72 h changing medium with fresh TSA every day. To analyze replication patterns, cells were pulse labeled with 100 μM BrdU or 5 μM EdU for 30 min. Cells were fixed for immunofluorescence in 4% formaldehyde for 10 min at RT.

Immunofluorescence

Cells were permeabilized with 0.5% Triton X-100 for 20 min at RT followed by immunostaining as published (27). For detection of PCNA, incubation for 10 min in ice-cold methanol after formaldehyde fixation was necessary. Acetylated histones were detected with rabbit anti-H4K8Ac antibodies (1/200, Upstate, Lake Placid, USA) in 4% BSA for 1 h at 37°C (Figure 1B). Incorporated BrdU was recognized by mouse anti-BrdU antibody (5 μg/ml, Becton Dickinson, Franklin Lakes, USA) in conjunction with 10 μg/μl DNase for 1 h at 37°C in 1% BSA/30 mM Tris HCl (pH 8.1)/0.33 mM $MgCl_2$/1 mM mercaptoethanol. Cells were then washed with 0.5% BSA/1 mM EDTA/PBS + 0.01% Tween to stop DNase digestion. EdU was detected using ClickIT chemistry (Invitrogen, Carlsbad, CA, USA) as described in (28). DNA was counterstained with DAPI for 10 min at RT (1 μg/ml, Sigma-Aldrich). Following secondary antibodies were used: Streptavidin-Alexa 488, 1/500 (Invitrogen), donkey-anti-mouse IgG-Cy3 and donkey-anti-rabbit IgG-Cy3 1/200 (The Jackson Laboratory, Bar Harbor, USA), goat-anti-mouse IgG-Alexa 488 1/200 (Invitrogen).

Immuno-FISH

Immuno-FISH was performed as described (29) using mouse-anti-PCNA (1/200, Dako, Carpinteria, USA, Figure 4), rabbit-anti-H4K8ac (1/200, Upstate, Cat. no. 06-760, Figure 3) antibodies and DNA probes against mouse repetitive sequences that were labeled with biotinylated dUTPs by nick translation. FISH signal was detected using Streptavidin-Cy5 1/500 (Amersham Biosciences, Piscataway, USA).

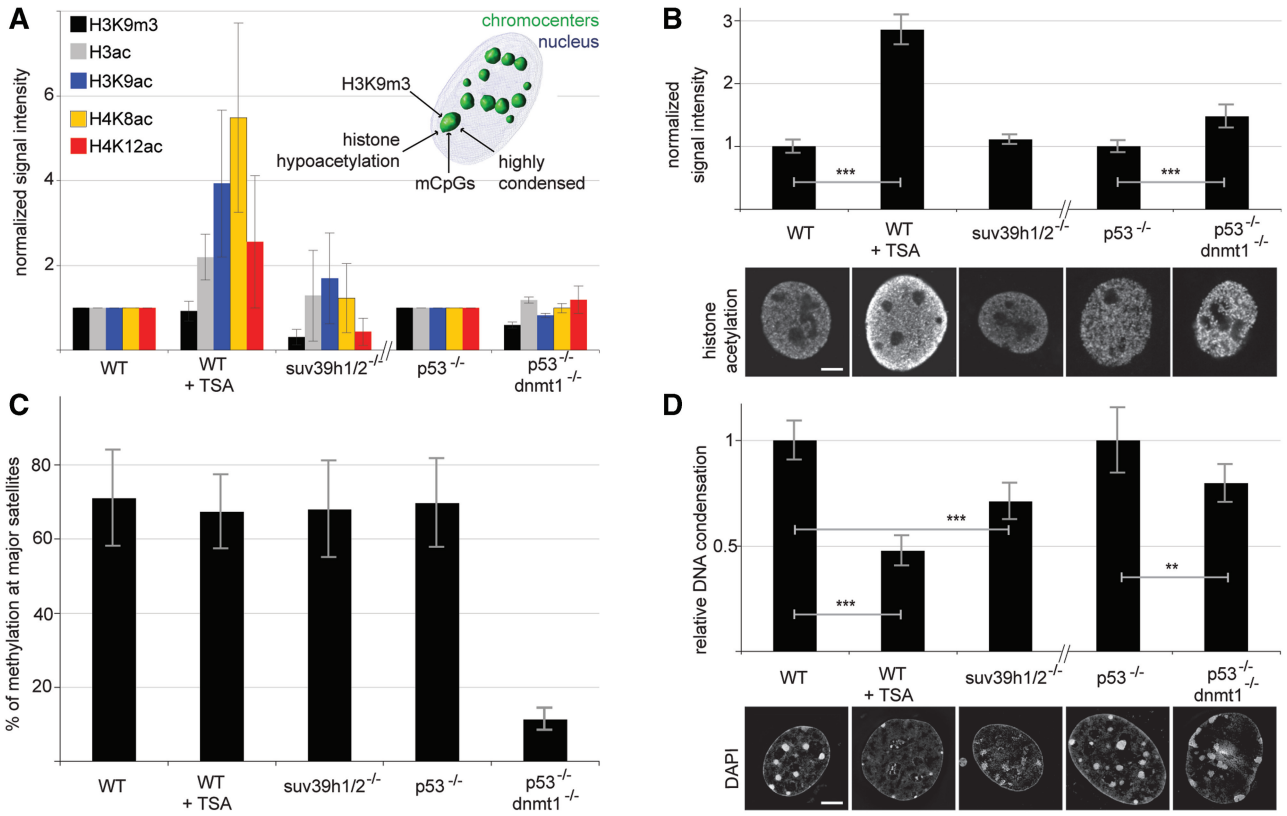

Figure 1. Manipulation of chromatin marks and organization of constitutive heterochromatin. Global histone acetylation levels were assessed by (**A**) western blot analysis of H3, H3ac, H3K9ac, H4, H4K8ac and H4K12ac, as well as (**B**) immunofluorescence *in situ* using antibodies against H4K8ac. Confocal mid-sections of *in situ* stainings were imaged and the mean value of the fluorescence signal was plotted as a ratio to control cells (MEF WT and $p53^{-/-}$, respectively). For western blot analysis, the fluorescence signal of histone modifications was double normalized to the amount of histone signal itself (H3 and H4, respectively), as well as to control cells. While TSA treatment resulted in a clear increase of histone acetylation, $dnmt1^{-/-}$ showed a slight increase in the level of global histone acetylation (**B**). On the other hand, $suv39h1/2^{-/-}$ exhibited, as expected, decreased levels of H3K9m3 (A). (**C**) Pyrosequencing analysis after bisulfite conversion demonstrated that exclusively $dnmt1^{-/-}$ had abnormal levels of DNA methylation at major satellites, decreased from 70% to 10%. (**D**) Mid-confocal sections of cells stained with DAPI were used to quantify the standard deviation of DAPI histograms, as a measure for the homogeneity of DNA compaction over the nucleus (see Supplementary Figure S5). The results, presented as a ratio to control cells, showed the effect of the different modifications on condensation of constitutive heterochromatin. High resolution 3D-SIM images are presented to illustrate how the disruption of all three factors, histone hypoacetylation, H3K9m3 and DNA methylation, resulted in changes in the structural conformation of chromocenters, with TSA having the most prominent effect, as seen by a more homogeneous DAPI staining. Error bars represent (A) standard deviation, (B–D) 95% CI. Statistical significance was tested by two-tailed *t*-test. $^{**}P < 0.01$; $^{***}P < 0.001$. Scale bar: 5 µm.

Western blot analysis and quantification

Cells were harvested, boiled in 1× Laemmli sample buffer and analyzed on western blots using the following primary antibodies (Figure 1A): rabbit-anti-H3 (1/5000, Upstate, Cat #: 07-690), rabbit-anti-H4 (1/1000, Upstate, Cat #: 07-108), rabbit-anti-H3ac (1/500, Upstate, Cat #: 06-599), rabbit-anti-H3K9ac (1/500, Upstate, Cat #: 06-942), rabbit-anti-H4K8ac, dilution 1/1000 (Upstate, Cat #: 06-790) and rabbit-anti-H4K12ac (1/1000, provided by T. Jenuwein). The following secondary antibodies were used: anti-rabbit IgG-Alexa Fluor 647 and anti-rabbit IgG-Alexa Fluor 680 (1/4000, Invitrogen). Blots were imaged using 700 nm excitation and quantified on a LI-COR Odyssey Infrared Imaging System using Odyssey V1.2.15 software (Biosciences, Lincoln). Integrated pixel intensity was measured for each band and the respective background signal was subtracted. Signals were normalized to the respective loading control (histone H3 or histone H4) and the fold difference to the respective control cells was calculated using Excel software (Microsoft, Redmont, USA).

Bisulfite treatment and pyrosequencing

Genomic DNA extraction was performed using QIAmp DNA extraction kit (Qiagen, Valencia, USA) according to the manufacturer's instructions. Bisulfite conversion of 1.5 µg DNA per sample was performed using EpiTect (Qiagen). Major satellite repeats were amplified by polymerase chain reaction using the following primers: AAAA TGAGAAATATTTATTTG (forward) and CCATGATT TTCAGTTTTCTT (reverse). Three amplification reactions were pooled together and sent for pyrosequencing to Varionostic (Ulm, Germany). Two pyrosequencing reactions, from the 3′- and 5′-end respectively, were performed per sample in order to cover the eight CpGs on each major satellite unit (Figure 1C and Supplementary Figure S1).

Microscopy

3D z-stacks of fixed cells were acquired with a Leica TCS SP5 confocal laser scanning microscope (Leica Microsystems, Wetzlar, Germany) using a HCX PL APO 63×/1.40 N.A. oil objective and laser lines at 405 nm, 488 nm, 561 nm and 633 nm. To accurately compare the treated cells between different experiments, all images were taken using identical settings. High-resolution DAPI images were acquired and reconstructed with 3D structured illumination microscopy as described in Ref. (30). Quantification of S-phase patterns was performed by epifluorescence microscopy using an Axiovert 200 microscope with a 63×/1.4 Plan-Apochromatic oil objective (Zeiss, Jena, Germany) equipped with a Sensicam 12-bit CCD camera system (PCO, Kelheim, Germany).

For additional colocalization analysis of early replication sites and chromocenters, 3D z-stacks of cells were collected using a Delta Vision Olympus wide-field microscope with a 60×/1.4 Plan-Apochromatic oil objective (Olympus Corp., Tokyo, Japan) and post-processed by deconvolution (Applied Precision, Issaquah, USA). For this, we used a radially averaged PSF recorded on the microscope under comparable image conditions.

Time-lapse microscopy

Cells were transfected with mRFP-PCNA (31) and MaSat-GFP (32) using Amaxa (Lonza, Cologne, Germany) nucleofection (solution V, program B-032) and thereby plated on 35 µ optical dishes (Ibidi, Munich, Germany). Time lapse microscopy was performed on an UltraView spinning disc system (PerkinElmer, UK) equipped with temperature, humidity and CO_2 incubation control (PeCon, Erbach, Germany). 3D z-stacks were acquired using a 63×/1.4 Plan-Apochromatic oil (Zeiss) every 30 min over up to 40 hours (Figure 5, Supplementary Figure S4 and Supplementary Movies 1–2).

Image analysis and quantification

Fluorescence intensity histogram quantifications were performed using ImageJ (http://rsb.info.nih.gov/ij/). A ROI was selected around each nucleus and the fluorescence intensity histogram of each nucleus, its mean value and standard deviation were measured. To quantify the levels of histone acetylation the mean values of the histograms of approx. 25 cells per condition were averaged and normalized to untreated cells (Figure 1B). These measurements were performed in triplicates.

To quantify the decondensation of pericentric heterochromatin the standard deviation of DAPI histograms of approximately 25 cells per condition were averaged and normalized to the control (see Supplementary Figure S5). The same analysis was repeated on three independent experiments and averaged (Figure 1D).

The frequency of early versus late replicating patterns (Figure 2 and Supplementary Figure S2) was quantified by counting only early and late replicating cells (sum of both equals n) and calculating the percentage of early or late patterns, respectively. Early replicating patterns are

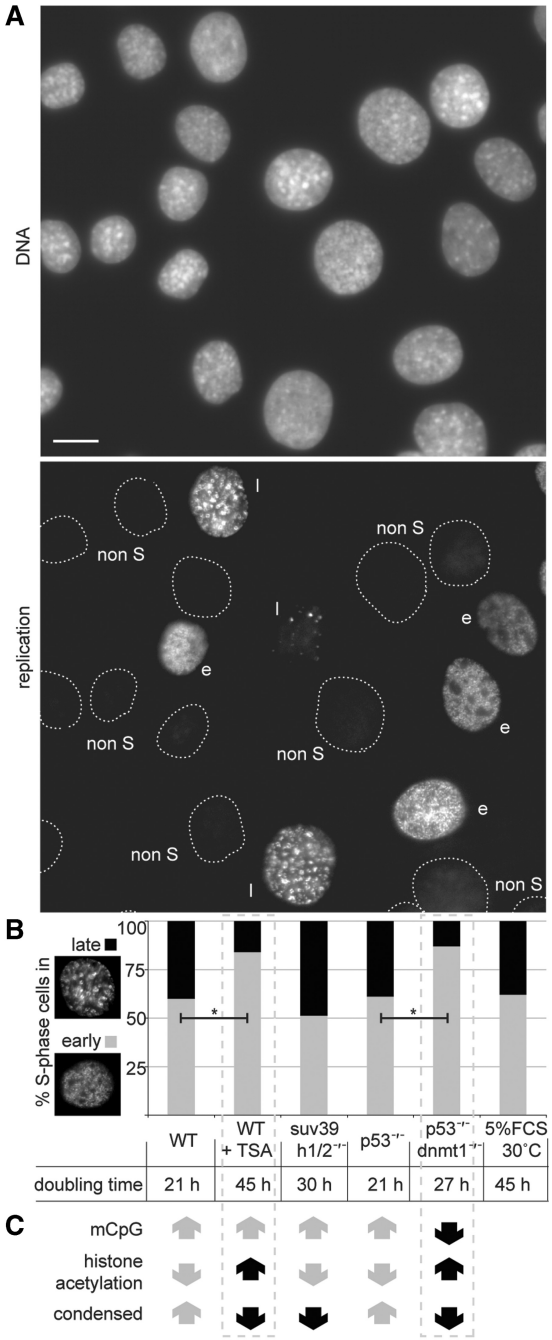

Figure 2. Effects of histone hyperacetylation, loss of H3K9 trimethylation and DNA methylation on late replication. Modified nucleotides (BrdU or EdU) were given to the cells for 30 min before fixation. Detection thereof and epifluorescence microscopy allowed the quantification of early versus late replication patterns. (**A**) An exemplary field in a control cell population, with cells going through early (e), late (l) S-phase, as well as not replicating (non S). (**B**) The distribution of early versus late replication patterns. In control cells, ~40% of replicating cells are going through late S. While *suv39h1/2*$^{-/-}$ did not show any significant effect on this distribution, both TSA-treated cells and *dnmt1*$^{-/-}$ exhibited a significant decrease in the frequency of late patterns down to ~15%. Statistical significance was tested using the Fisher's exact test. The doubling time of the control, mutant and treated cells are shown below the histogram. Cells grown under starvation conditions have a similar doubling time as TSA treated cells, even though the replication pattern distribution of the former is unchanged. (**C**) Summarizes the chromatin changes in the different cells. Black arrows indicate differences to the respective control cells. Scale bar: 10 µm.

characterized by foci distributed homogenously throughout the nucleus with exception of the nuclear and nucleolar periphery. Late replication patterns are clearly recognizable due to the appearance of fewer but larger clusters of a couple of hundreds replication foci (2–6).

Colocalization of major satellites and early replication sites (Figure 4A and Supplementary Figure S3) was calculated using custom written software in the Priithon image analysis platform (http://code.google.com/p/priithon/). Images were processed using a 3D median filter for chromocenters and 3D Gaussian-of-Laplace filter for replication foci. Filtered images were thresholded automatically using the Otsu algorithm (33). The thresholded images were used to calculate the colocalization percentage. For this, the number of all overlapping voxels was divided by the total number of voxels corresponding to chromocenter signals.

The total histone acetylation signal at the chromocenters (Figure 3) was quantified as described above, but after obtaining a mask for the acetylation channel this was multiplied by the raw acetylation image. The intensity of all remaining voxels was then summed up.

The rate of DNA synthesis (Figure 4B) was quantified by measuring the integrated intensity of newly replicated DNA signal throughout the nucleus in cells pulse-labeled for 15 min with EdU.

S-phase length (Figure 4C) was calculated from the percentage of S-phase cells in an asynchronous population and the total cell cycle duration.

Colocalization of replication foci and major satellites on live cell data was assessed by the H-coefficient (Figure 5 and Supplementary Figure S4B), using the following formula:

$$H_{\text{coeff}} = \frac{N_p \sum_{i=1}^{N_p} Ir_i \, Ig_i}{\left(\sum_{i=1}^{N_p} Ir_i\right)\left(\sum_{i=1}^{N_p} Ig_i\right)},$$

where Ir_i and Ig_i is the intensity of the channels r and g in the pixel i and Np is the total number of pixels.

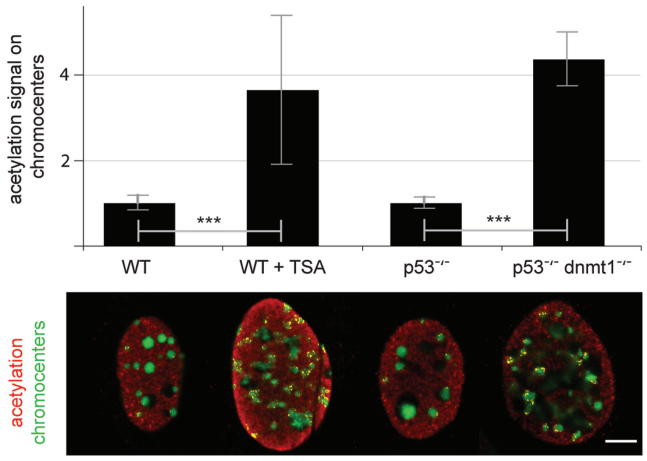

Figure 3. *Dnmt1*$^{-/-}$ have increased levels of histone acetylation at chromocenters. Co-staining of histone acetylation and chromocenters by immuno-FISH and 3D confocal imaging (upper panel) allowed us to quantify the total histone acetylation signal on the chromocenters (lower panel). As expected, TSA treatment resulted in a clear increase of histone acetylation in these regions. Interestingly, lowering the levels of DNA methylation at chromocenters by knocking out *dnmt1*$^{-/-}$ had the same effect on histone acetylation, pointing to the fact that this modification is most likely to control late replication of constitutive heterochromatic regions. Error bars represent 95% CI. Statistical significance was tested by two-tailed *t*-test. ***$P < 0.001$. Scale bar: 5 µm.

RESULTS

Manipulation of the composition of constitutive heterochromatin

In order to investigate the connection between chromatin markers and replication timing, we used drug treatment and genetically modified cell lines to manipulate the main features of constitutive heterochromatin: histone hypoacetylation, accumulation of H3K9m3 and DNA methylation. We treated wild type mouse embryonic fibroblasts (MEF-WT) with TSA to inhibit HDACs (34), thereby elevating histone acetylation. To modulate the levels of H3K9m3 on constitutive heterochromatin, we performed experiments in *suv39h1/2* double knock-out cells (35), which lack the enzymes responsible for this modification. Finally, we used *dnmt1*$^{-/-}$ cells (25), with low levels of DNA methylation. Since *dnmt1*$^{-/-}$ somatic cells do not proliferate normally, these experiments were performed in homozygous *p53*$^{-/-}$ cells to increase their viability. As a control for the *p53*$^{-/-}$/*dnmt1*$^{-/-}$ double knock-out cells, we used *p53*$^{-/-}$ cells (25).

Changes in the levels of chromatin markers were assessed by western blot analysis of cell extracts (Figure 1A), as well as immunofluorescence stainings *in situ* (Figure 1B) using antibodies specific to the histone modifications of interest. These data confirmed that TSA treatment promoted an increase of histone acetylation and that *suv39h1/2*$^{-/-}$ cells have a decreased level of H3K9m3. *Dnmt1*$^{-/-}$ cells lost DNA methylation at major satellite repeats, as shown by pyrosequencing analysis after bisulfite conversion (Figure 1C and Supplementary Figure S1). In the case of TSA treatment and *suv39h1/2*$^{-/-}$ cells, the effects on the chromatin modifications were specific; TSA-treatment only affected histone acetylation and *suv39h1/2*$^{-/-}$ cells exhibited only significant alterations in histone methylation. In contrast, *dnmt1*$^{-/-}$ cells, in addition to a drastic decrease in DNA methylation, also exhibited an increase in global histone acetylation (Figure 1B and see below). This result is consistent with the idea that cross-talk exists between markers at constitutive heterochromatin, and that disrupting one modification may promote alterations in the overall chromatin composition and state of the region (36).

Moreover, we predict that disruption of these three chromatin modifications may also influence the condensation levels of chromocenters (37). Figure 1D illustrates that chromocenters in control cells exhibit the characteristic round, condensed structure described above.

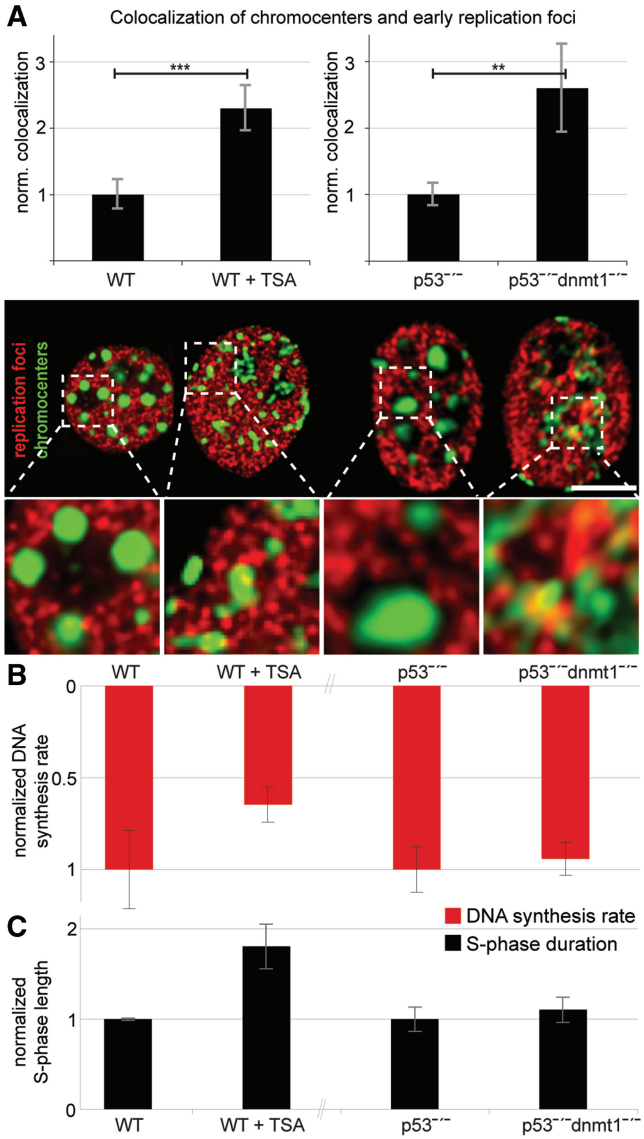

Figure 4. Histone hyperacetylation at heterochromatic regions increase their replication concomitant to euchromatin. (**A**) Immuno-FISH was performed to co-stain replication structures (by either PCNA or EdU) and chromocenters. Early patterns were selected and imaged by 3D confocal microscopy, as well as deconvolution microscopy. ROIs were defined automatically in the chromocenter channel by the Otsu algorithm and used to quantify the replication signal at chromocenters. The percentage of chromocenter material colocalizing with early replication foci was plotted as ratio to control cells. Both, TSA-treated and *dnmt1*$^{-/-}$ cells showed a significant increase of replication of heterochromatic sequences during early S-phase. (**B**) Inverted graph of DNA synthesis rate measured by quantifying the integrated intensity of modified nucleotides incorporated during a 15-min pulse imaged as 3D confocal stacks ($n > 90$). (**C**) S-phase length normalized to control cells showing that the length of S-phase is anti-correlated to DNA synthesis rate. Error bars represent 95% CI (A and B) or standard deviation (C). Statistical significance was tested by two-tailed *t*-test. $^{**}P < 0.01$; $^{***}P < 0.001$. Scale bar: 5 μm.

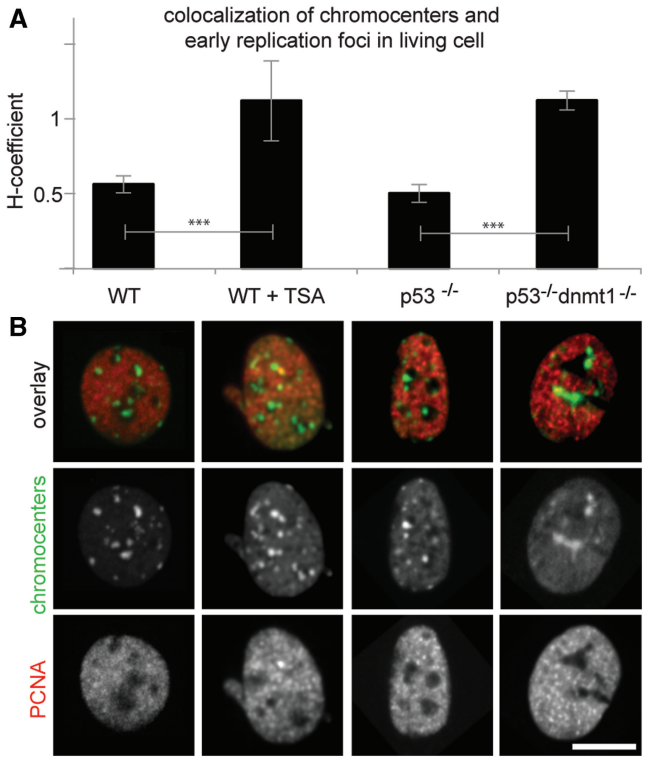

Figure 5. Histone acetylation causes earlier onset of replication of constitutive heterochromatic regions. Progression of S-phase was followed by time-lapse microscopy of living cells transfected with mRFP-PCNA, marking sites of active replication, and MaSat-GFP, labeling major satellite repeats. The temporal information gained by this approach allowed us to unequivocally select cells going through early S-phase and quantify the colocalization of constitutive heterochromatic regions and replication structures prior to the onset of late replication. (**A**) Hyperacetylated chromosomes showed a significantly increased colocalization with PCNA during early S-phase when compared to untreated wild-type cells. (**B**) Exemplary images of wild type cells going through early S-phase. The TSA-treated cell (bottom row) clearly shows colocalization of chromocenters and TSA. Error bars represent 95% CI. Statistical significance was tested by two-tailed *t*-test. $^{***}P < 0.001$. Scale bars: 5 μm.

In contrast, this pattern is disrupted after TSA treatment, as well as in *suv39h1/2*$^{-/-}$ and *dnmt1*$^{-/-}$ cells. Chromocenters in these cells appeared more open and lacked the distinct, highly condensed appearance of control cells. Since the decondensation of constitutive heterochromatin results in a more homogenous DNA staining throughout the nucleus, we measured the standard deviation of the respective DAPI histograms to quantify the degree of decondensation in treated and mutant cells (Figure 1D). Since all three treatments influence chromatin condensation, any differences in the effects on replication timing resulting from TSA treatment or knocking out *dnmt1* or *suv39h1/2* would exclude condensation as a primary determinant of replication timing.

Manipulating chromatin epistate affects late replication of constitutive heterochromatin

If changes in the composition of constitutive heterochromatin promote alterations in its replication timing, we predict that the stereotypical late replication timing exhibited by constitutive heterochromatin would be disrupted. To test this model, we quantified the percentage of late replication patterns in S-phase cells. Modified

nucleotides, either 5-bromo-2-deoxyuridine (BrdU) or 5-ethynyl-2′-deoxyuridine (EdU), were added to proliferating populations of cells and incorporated into newly synthesized DNA for 30 min prior to fixation. Detection of these nucleotides allowed us to quantify the percentage of replicating cells going through late S-phase, as defined by the characteristic pattern formed by large replication structures as compared to early S-phase patterns (Figure 2A). One caveat of this experiment is that several of the treatments we use increase the time required for the cells to complete the cell cycle. To ensure that the increased duplication time in mutant and treated cells does not result in a change of the replication pattern distribution, we cultivated wild-type fibroblasts under decreased temperature and serum concentration (30°C, 5% FCS). While these cells progressed much slower through the cell cycle, similarly to TSA treated cells, we did not observe any difference in the distribution of replication patterns when compared to the control cells grown under standard conditions (Figure 2B). In an untreated wild-type population, ~40% of replicating cells exhibited staining patterns consistent with late replication (Figure 2B). While *suv39h1/2*$^{-/-}$ did not show a significant change in this distribution, in agreement with previous data (38), both TSA-treated cells and *dnmt1*$^{-/-}$ cells exhibited a clear decrease (down to 15%) in the frequency of late replication patterns. These results demonstrate that manipulation of either histone acetylation or DNA methylation leads to an alteration in the distribution of late replication patterns, suggesting a possible change in the replication timing of heterochromatic regions.

Before investigating how these two chromatin modifications are related to the regulation of replication timing, it was important to dissect the relationship between histone acetylation and DNA methylation at chromocenters (39). We showed that TSA had no effect on DNA methylation at heterochromatic sequences (Figure 1C), while *dnmt1*$^{-/-}$ cells exhibited increased levels of global histone acetylation (Figure 1A and B). It is therefore possible that the effect of reducing DNA methylation on replication timing is directly related to the accompanying effect on histone acetylation (40). However, since the increase in the global level of histone acetylation in *dnmt1*$^{-/-}$ cells was not as pronounced as in TSA-treated cells (Figure 1A and B), we refined our analysis to directly examine the levels of histone acetylation at heterochromatic regions.

We used immuno-FISH to measure changes in histone acetylation levels specifically at chromocenters, simultaneously detecting histone acetylation by immunostaining, and chromocenters by FISH. In contrast to the unspecific DNA staining by DAPI, FISH of major satellite repeats clearly labels these regions based on their genetic composition and independently of their condensation level. Subsequent collection of 3D confocal stacks allowed us to quantify the total acetylation signal at chromocenters (Figure 3). TSA treatment resulted in a clear increase of histone acetylation at heterochromatic regions with no change in DNA methylation. Strikingly, *dnmt1*$^{-/-}$ cells showed the same degree of hyperacetylation at chromocenters. Furthermore, treating *dnmt1*$^{-/-}$ cells with TSA as done for WT MEF did not reduce the frequency of late replicating patterns (Supplementary Figure S2). The fact that TSA treatment of *dnmt1*$^{-/-}$ cells does not result in additional effects on their replication timing indicates that chromocenters in *dnmt1*$^{-/-}$ cells have lost normal histone hypoacetylation. It further suggests that the hyperacetylation observed in *dnmt1*$^{-/-}$ cells may be functionally equivalent to that in TSA-treated cells.

Dnmt1$^{-/-}$ cells provide a drug-free system in which histone acetylation is specifically increased at otherwise methylated regions, such as pericentromeric heterochromatin. We have thus utilized two distinct approaches to promote the hyperacetylation of constitutive heterochromatin. In both cases, we observe a decrease of late replication patterns, raising the question of when these hyperacetylated heterochromatic regions are being replicated. Therefore, one possible model would be that hyperacetylation of heterochromatin promotes earlier onset of replication.

Histone hypoacetylation of constitutive heterochromatin is required for its late replication

To test the hypothesis that hyperacetylated heterochromatic sequences are replicated during early S-phase, we examined whether there was an increase of replication sites at heterochromatic regions during early S-phase. To this end, we used immuno-FISH to co-stain replication sites and chromocenters and directly examine their interaction during early S-phase. In control cells, as expected, we detected very little association between heterochromatin and sites of early DNA replication. In contrast, both TSA-treated and *dnmt1*$^{-/-}$ cells exhibited increased colocalization between chromocenters and early replication foci (Figure 4). Additionally, we analyzed the level of colocalization per chromocenter to assess whether the increased early replication of hyperacetylated heterochromatic regions reflected single chromocenters being entirely replicated during early S-phase or a general increase of early replication distributed equally throughout all chromocenters. This analysis demonstrated that the shift to early replication is well distributed throughout chromocenters, with a significant decrease in the percentage of chromocenters showing <10% overlap with early replication foci from ~40% of all chromocenters in control cells to <20% of all chromocenters in both TSA-treated and *dnmt1*$^{-/-}$ cells. However, we also found a small percentage of chromocenters that are replicated mostly during early S-phase (Supplementary Figure S3). These results support the notion that hyperacetylated constitutive heterochromatic regions are being replicated in parallel to euchromatin, i.e. during early S-phase.

To test if histone acetylation might result in faster replication fork progression, we quantified the rate of DNA synthesis in TSA-treated and dnmt1$^{-/-}$ versus control cells. To this end, the total amount of modified nucleotides incorporated by replicating cells during a 15-min pulse was measured in confocal 3D stacks (Figure 4B). The outcome of this analysis demonstrated that in fact, DNA synthesis is slowed down in treated cells rather than accelerated, and this corresponds to their longer S-phase (Figure 4C). Importantly, these observations

rendered the increased colocalization of early replication foci and heterochromatic regions observed in TSA-treated and *dnmt1*$^{-/-}$ cells even more significant. Interestingly, neither TSA treatment nor knocking out *dnmt1* resulted in checkpoint activation, as measured by Chk1 phosphorylation, while our positive control of UV-C irradiated MEFs showed clear phosphorylation of Chk1 (data not shown). These observations rule out the possibility that the described shift in replication dynamics would result from checkpoint activation.

To further investigate the idea that increased histone acetylation correlates with a shift in the replication timing of heterochromatin, we monitored S-phase progression in living cells, focusing again on the association between constitutive heterochromatin and the replication machinery. Cells were transfected with mRFP-PCNA, a central component of the replication machinery (3,31), and MaSat-GFP, a polydactyl zinc-finger protein which binds to major satellite repeats (32) and is a live-cell marker for pericentromeric heterochromatin. Series of time-lapse images were collected in 30-min intervals for up to 45 h (Supplementary Movies 1–2 and Figure S4A). Observation over such long periods allowed us to distinguish between the different stages of S-phase in the same cell and to unequivocally identify cells in early S-phase. We analyzed the level of colocalization between replication foci and major satellites and observed a clear increase of colocalization between early replication foci and major satellites as a consequence of TSA treatment and in *dnmt1*$^{-/-}$ cells (Figure 5 and Supplementary Figure S4). Based on these results, we conclude that increasing histone acetylation at constitutive heterochromatic regions, results in an earlier onset of replication. We therefore propose that histone hypoacetylation is indispensable for maintenance of the late-replication timing of constitutive heterochromatin.

DISCUSSION

In this study, we used drug treatment and mutant cell lines to comprehensively assess which chromatin modifications are important for defining the late replicating nature of constitutive heterochromatin. By combining these approaches with quantitative microscopy, we were able to directly investigate the connection between chromatin modifications and the spatial and temporal control of replication timing. We show that treatment with TSA, as well as knocking out *dnmt1*, results in an earlier onset of replication at chromocenters. In both cases, this effect was associated with an increase in the normal levels of histone acetylation at chromocenters (see below and Figure 6). In contrast, *suv39h1/2*$^{-/-}$ cells with reduced levels of H3K9m3 and normal levels of histone acetylation exhibited no change in replication timing. These data therefore suggest that the level of histone acetylation at a given genomic region is a major factor in determining its replication timing.

One important consideration when manipulating the chromatin state of any genomic region is the downstream effects on chromatin structure and the binding of additional chromatin factors. This is particularly relevant with chromocenters, given that their DNA and histone modifications are directly related to their highly condensed nature and contributes to the recruitment of multiple proteins (41). In this case, the methods we used to perturb the molecular markers of constitutive heterochromatin (i.e. TSA treatment, *dnmt1* and *suv39h1/2* knock-outs) all resulted in a large-scale decondensation of the chromocenters. However, only two out of the three cases promoted a shift in the replication timing of the constitutive heterochromatin. The fact that *suv39h1/2*$^{-/-}$ cells exhibit no clear change in their replication timing indicates that the chromatin decondensation we observe here is not directly related to an alteration in replication timing. While it has been reported that an open chromatin condensation may facilitate early replication (42), we argue that a general decondensation on the scale that is visualized by DAPI staining *in situ* is not *per se* sufficient to promote early replication of heterochromatic regions. It should be stressed here that it is very likely that there are more subtle local differences in chromatin compaction and structure, which cannot be

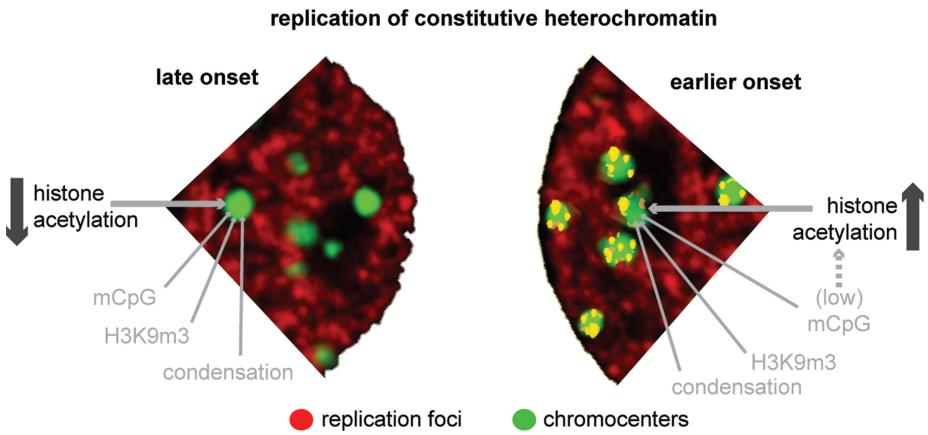

Figure 6. Summary of the effect of chromatin changes in replication timing. Histone hyperacetylation at constitutive heterochromatic regions results in earlier replication onset. While DNA methylation has an indirect effect on replication timing via histone acetylation (dashed arrow), both H3K9m3 accumulation and large-scale decondensation of chromocenters are not sufficient to disrupt late replication.

detected by a mere DAPI staining and might affect replication timing, possibly by increasing accessibility of, e.g. replication factors to DNA. Knocking out *suv39h1/2* genes also abolishes the binding of HP1 to chromocenters (35), indicating that this important heterochromatin determinant does not contribute to the regulation of replication timing. We, therefore, conclude that neither H3K9m3, nor large-scale chromatin condensation, nor HP1 binding, are directly involved in defining the late replication pattern observed for constitutive heterochromatin. Interestingly, knocking down HP1 in *Drosophila* affects late replication of heterochromatin, demonstrating that replication timing in mammalian cells underlies a somewhat different control mechanism as in invertebrates.

In both, TSA-treated and *dnmt1*$^{-/-}$ cells, we observe a shift in replication timing, whereby normally late replicating constitutive heterochromatin is replicated during early S-phase. TSA treatment directly promotes the hyperacetylation of histones, specifically relating this chromatin modification to the regulation of replication timing. As DNA methylation is unaffected in TSA-treated cells, we conclude that this DNA modification does not block early replication. While DNA methylation loss is the most direct effect of knocking out *dnmt1*, our results (Figure 3), as well as previous studies (43), demonstrate that this decrease leads to elevated histone acetylation levels at chromocenters. We therefore argue that in *dnmt1*$^{-/-}$ cells, concomitant changes in the level of histone acetylation are involved in the shift in replication timing of constitutive heterochromatin, analogous to what we observe in TSA-treated cells. Nonetheless, we cannot strictly exclude the possibility that TSA-mediated acetylation of non-histone proteins or that knocking out *dnmt1* might have other secondary effects, which could play a role in the described shift in replication timing. However, the fact that two different strategies to manipulate the levels of histone acetylation, a chemical and genetic one, result in similar effects on replication timing, strongly suggests that histone hyperacetylation is involved in promoting earlier replication onset of constitutive heterochromatin. Thus, we propose that histone hypoacetylation facilitates late replication timing independently of both histone methylation and DNA methylation (Figure 6). Interestingly, our results show that there is no mechanism absolutely preventing early replication of heterochromatic regions. Indeed, we have reported that in normal untreated mouse cells, a certain small percentage of the usually late-replicating centromeric regions replicate during early S-phase (8).

Ultimately, replication timing is defined by the timing of origin firing. The relative efficiency model of origin firing proposes that early origins fire more efficiently, while late origins have a low efficiency at the beginning of S-phase, which increases as S-phase progresses, thus assuring that potential gaps of unreplicated DNA are closed in a timely fashion (44). In the context of this model, our data suggest that histone acetylation directly or indirectly plays an important role in defining the firing efficiency of origins and concomitantly the replication timing of distinct genomic regions. There are various processes leading to origin firing itself at which histone acetylation might regulate replication timing. For instance, it has been shown recently that origin firing dynamics in fission yeast can be a result of differences in the time of ORC binding at different regions (45). The binding of limiting ORC factors could be enhanced at acetylated regions with an open chromatin conformation. Origin licensing is another process that can be enhanced by histone acetylation, since HBO1-mediated histone acetylation in yeast has been shown to play an important role in the loading of the Mcm 2–7 complex (46), necessary for origin licensing (47). An increased basal level of histone acetylation may therefore facilitate origin licensing. Alternatively, histone acetylation could also play a role in the actual firing process, potentially by increasing accessibility or binding affinity to limiting firing factors, such as yeast Cdc45 (20,48), which has been shown to increase the firing efficiency of inefficient origins (45). Further experiments using high-resolution microscopy could give a more detailed insight into the structural changes resulting from histone hyperacetylation. Moreover, protein–DNA interaction profiling under different chromatin acetylation conditions could elucidate how this histone modification affects binding of licensing/firing factors to origins and how chromatin state influences genome metabolism.

SUPPLEMENTARY DATA

Supplementary Data are available at NAR Online.

ACKNOWLEDGEMENTS

We thank T. Jenuwein for providing the *suv39h1/2*$^{-/-}$ and wild type MEFs, H. Cedar for the *p53*$^{-/-}$ and *p53/dnmt1*$^{-/-}$ MEFs. B. J. Van der Zaal for the GFP-tagged MaSat construct, H. Saumweber for usage of the Deltavision microscopy system, A. Maiser for acquisition of high-resolution microscopy images, S. Goerisch and V. O. Chagin for discussions, J. Bolius for help with stainings and Anne Lehmkuhl for excellent technical work.

FUNDING

Funding for open access charge: BioImaging Network and the Nanosystems Initiative Munich (to H.L.); Deutsche Forschungsgemeinschaft (Ca198/7-1, Ca198/3-3, SFB740/TPA1 to M.C.C.).

Conflict of interest statement. None declared.

REFERENCES

1. Craig,J.M. and Bickmore,W.A. (1993) Chromosome bands–flavours to savour. *Bioessays*, **15**, 349–354.
2. Baddeley,D., Chagin,V.O., Schermelleh,L., Martin,S., Pombo,A., Carlton,P.M., Gahl,A., Domaing,P., Birk,U., Leonhardt,H. *et al.* (2010) Measurement of replication structures at the nanometer scale using super-resolution light microscopy. *Nucleic Acids Res.*, **38**, e8.
3. Leonhardt,H., Rahn,H.P., Weinzierl,P., Sporbert,A., Cremer,T., Zink,D. and Cardoso,M.C. (2000) Dynamics of DNA replication factories in living cells. *J. Cell Biol.*, **149**, 271–280.

4. Fox,M.H., Arndt-Jovin,D.J., Jovin,T.M., Baumann,P.H. and Robert-Nicoud,M. (1991) Spatial and temporal distribution of DNA replication sites localized by immunofluorescence and confocal microscopy in mouse fibroblasts. *J. Cell Sci.*, **99(Pt 2)**, 247–253.
5. Nakamura,H., Morita,T. and Sato,C. (1986) Structural organizations of replicon domains during DNA synthetic phase in the mammalian nucleus. *Exp. Cell Res.*, **165**, 291–297.
6. van Dierendonck,J.H., Keyzer,R., van de Velde,C.J. and Cornelisse,C.J. (1989) Subdivision of S-phase by analysis of nuclear 5-bromodeoxyuridine staining patterns. *Cytometry*, **10**, 143–150.
7. O'Keefe,R.T., Henderson,S.C. and Spector,D.L. (1992) Dynamic organization of DNA replication in mammalian cell nuclei: spatially and temporally defined replication of chromosome-specific alpha-satellite DNA sequences. *J. Cell Biol.*, **116**, 1095–1110.
8. Weidtkamp-Peters,S., Rahn,H.P., Cardoso,M.C. and Hemmerich,P. (2006) Replication of centromeric heterochromatin in mouse fibroblasts takes place in early, middle, and late S phase. *Histochem. Cell Biol.*, **125**, 91–102.
9. Muck,J. and Zink,D. (2009) Nuclear organization and dynamics of DNA replication in eukaryotes. *Front Biosci.*, **14**, 5361–5371.
10. Vashee,S., Cvetic,C., Lu,W., Simancek,P., Kelly,T.J. and Walter,J.C. (2003) Sequence-independent DNA binding and replication initiation by the human origin recognition complex. *Genes Dev.*, **17**, 1894–1908.
11. Lin,C.M., Fu,H., Martinovsky,M., Bouhassira,E. and Aladjem,M.I. (2003) Dynamic alterations of replication timing in mammalian cells. *Curr. Biol.*, **13**, 1019–1028.
12. Dazy,S., Gandrillon,O., Hyrien,O. and Prioleau,M.N. (2006) Broadening of DNA replication origin usage during metazoan cell differentiation. *EMBO Rep.*, **7**, 806–811.
13. Hiratani,I., Ryba,T., Itoh,M., Yokochi,T., Schwaiger,M., Chang,C.W., Lyou,Y., Townes,T.M., Schubeler,D. and Gilbert,D.M. (2008) Global reorganization of replication domains during embryonic stem cell differentiation. *PLoS Biol.*, **6**, e245.
14. Rampakakis,E., Di Paola,D., Chan,M.K. and Zannis-Hadjopoulos,M. (2009) Dynamic changes in chromatin structure through post-translational modifications of histone H3 during replication origin activation. *J. Cell Biochem.*, **108**, 400–407.
15. Aladjem,M.I. (2007) Replication in context: dynamic regulation of DNA replication patterns in metazoans. *Nat. Rev. Genet.*, **8**, 588–600.
16. Schwaiger,M., Stadler,M.B., Bell,O., Kohler,H., Oakeley,E.J. and Schubeler,D. (2009) Chromatin state marks cell-type- and gender-specific replication of the Drosophila genome. *Genes Dev.*, **23**, 589–601.
17. Lande-Diner,L., Zhang,J. and Cedar,H. (2009) Shifts in replication timing actively affect histone acetylation during nucleosome reassembly. *Mol. Cell*, **34**, 767–774.
18. Jorgensen,H.F., Azuara,V., Amoils,S., Spivakov,M., Terry,A., Nesterova,T., Cobb,B.S., Ramsahoye,B., Merkenschlager,M. and Fisher,A.G. (2007) The impact of chromatin modifiers on the timing of locus replication in mouse embryonic stem cells. *Genome Biol.*, **8**, R169.
19. Kemp,M.G., Ghosh,M., Liu,G. and Leffak,M. (2005) The histone deacetylase inhibitor trichostatin A alters the pattern of DNA replication origin activity in human cells. *Nucleic Acids Res.*, **33**, 325–336.
20. Vogelauer,M., Rubbi,L., Lucas,I., Brewer,B.J. and Grunstein,M. (2002) Histone acetylation regulates the time of replication origin firing. *Mol. Cell*, **10**, 1223–1233.
21. Schwaiger,M., Kohler,H., Oakeley,E.J., Stadler,M.B. and Schubeler,D. (2010) Heterochromatin protein 1 (HP1) modulates replication timing of the Drosophila genome. *Genome Res.*, **20**, 771–780.
22. Heitz,E. (1928) Heterochromatin of the moss. I. *Jahrbücher für wissenschaftlitsche Botanik*, **69**, 762–818.
23. Jones,K.W. (1970) Chromosomal and nuclear location of mouse satellite DNA in individual cells. *Nature*, **225**, 912–915.
24. Vissel,B. and Choo,K.H. (1989) Mouse major (gamma) satellite DNA is highly conserved and organized into extremely long tandem arrays: implications for recombination between nonhomologous chromosomes. *Genomics*, **5**, 407–414.
25. Lande-Diner,L., Zhang,J., Ben-Porath,I., Amariglio,N., Keshet,I., Hecht,M., Azuara,V., Fisher,A.G., Rechavi,G. and Cedar,H. (2007) Role of DNA methylation in stable gene repression. *J. Biol. Chem.*, **282**, 12194–12200.
26. Peters,A.H., O'Carroll,D., Scherthan,H., Mechtler,K., Sauer,S., Schofer,C., Weipoltshammer,K., Pagani,M., Lachner,M., Kohlmaier,A. *et al.* (2001) Loss of the Suv39h histone methyltransferases impairs mammalian heterochromatin and genome stability. *Cell*, **107**, 323–337.
27. Cardoso,M.C., Leonhardt,H. and Nadal-Ginard,B. (1993) Reversal of terminal differentiation and control of DNA replication: cyclin A and Cdk2 specifically localize at subnuclear sites of DNA replication. *Cell*, **74**, 979–992.
28. Salic,A. and Mitchison,T.J. (2008) A chemical method for fast and sensitive detection of DNA synthesis in vivo. *Proc. Natl Acad. Sci. USA*, **105**, 2415–2420.
29. Zinner,R., Teller,K., Versteeg,R., Cremer,T. and Cremer,M. (2007) Biochemistry meets nuclear architecture: multicolor immuno-FISH for co-localization analysis of chromosome segments and differentially expressed gene loci with various histone methylations. *Adv. Enzyme Regul.*, **47**, 223–241.
30. Schermelleh,L., Carlton,P.M., Haase,S., Shao,L., Winoto,L., Kner,P., Burke,B., Cardoso,M.C., Agard,D.A., Gustafsson,M.G. *et al.* (2008) Subdiffraction multicolor imaging of the nuclear periphery with 3D structured illumination microscopy. *Science*, **320**, 1332–1336.
31. Sporbert,A., Domaing,P., Leonhardt,H. and Cardoso,M.C. (2005) PCNA acts as a stationary loading platform for transiently interacting Okazaki fragment maturation proteins. *Nucleic Acids Res.*, **33**, 3521–3528.
32. Lindhout,B.I., Fransz,P., Tessadori,F., Meckel,T., Hooykaas,P.J. and van der Zaal,B.J. (2007) Live cell imaging of repetitive DNA sequences via GFP-tagged polydactyl zinc finger proteins. *Nucleic Acids Res.*, **35**, e107.
33. Otsu,N. (1979) A threshold selection method from gray-level histograms. *IEEE Trans. Sys., Man., Cyber.*, **9**, 62–66.
34. Taddei,A., Maison,C., Roche,D. and Almouzni,G. (2001) Reversible disruption of pericentric heterochromatin and centromere function by inhibiting deacetylases. *Nat. Cell Biol.*, **3**, 114–120.
35. Lehnertz,B., Ueda,Y., Derijck,A.A., Braunschweig,U., Perez-Burgos,L., Kubicek,S., Chen,T., Li,E., Jenuwein,T. and Peters,A.H. (2003) Suv39h-mediated histone H3 lysine 9 methylation directs DNA methylation to major satellite repeats at pericentric heterochromatin. *Curr. Biol.*, **13**, 1192–1200.
36. Felsenfeld,G. and Groudine,M. (2003) Controlling the double helix. *Nature*, **421**, 448–453.
37. Popova,E.Y., Krauss,S.W., Short,S.A., Lee,G., Villalobos,J., Etzell,J., Koury,M.J., Ney,P.A., Chasis,J.A. and Grigoryev,S.A. (2009) Chromatin condensation in terminally differentiating mouse erythroblasts does not involve special architectural proteins but depends on histone deacetylation. *Chromosome Res.*, **17**, 47–64.
38. Wu,R., Singh,P.B. and Gilbert,D.M. (2006) Uncoupling global and fine-tuning replication timing determinants for mouse pericentric heterochromatin. *J. Cell Biol.*, **174**, 185–194.
39. Nan,X., Ng,H.H., Johnson,C.A., Laherty,C.D., Turner,B.M., Eisenman,R.N. and Bird,A. (1998) Transcriptional repression by the methyl-CpG-binding protein MeCP2 involves a histone deacetylase complex. *Nature*, **393**, 386–389.
40. Rountree,M.R., Bachman,K.E. and Baylin,S.B. (2000) DNMT1 binds HDAC2 and a new co-repressor, DMAP1, to form a complex at replication foci. *Nat. Genet.*, **25**, 269–277.
41. Dillon,N. and Festenstein,R. (2002) Unravelling heterochromatin: competition between positive and negative factors regulates accessibility. *Trends Genet.*, **18**, 252–258.
42. Aladjem,M.I., Groudine,M., Brody,L.L., Dieken,E.S., Fournier,R.E., Wahl,G.M. and Epner,E.M. (1995) Participation of the human beta-globin locus control region in initiation of DNA replication. *Science*, **270**, 815–819.
43. Jones,P.L., Veenstra,G.J., Wade,P.A., Vermaak,D., Kass,S.U., Landsberger,N., Strouboulis,J. and Wolffe,A.P. (1998) Methylated

DNA and MeCP2 recruit histone deacetylase to repress transcription. *Nat. Genet.*, **19**, 187–191.
44. Rhind,N. (2006) DNA replication timing: random thoughts about origin firing. *Nat. Cell Biol.*, **8**, 1313–1316.
45. Wu,P.Y. and Nurse,P. (2009) Establishing the program of origin firing during S phase in fission yeast. *Cell*, **136**, 852–864.
46. Miotto,B. and Struhl,K. (2010) HBO1 histone acetylase activity is essential for DNA replication licensing and inhibited by Geminin. *Mol. Cell*, **37**, 57–66.
47. Takahashi,T.S., Wigley,D.B. and Walter,J.C. (2005) Pumps, paradoxes and ploughshares: mechanism of the MCM2-7 DNA helicase. *Trends Biochem. Sci.*, **30**, 437–444.
48. Aparicio,O.M., Stout,A.M. and Bell,S.P. (1999) Differential assembly of Cdc45p and DNA polymerases at early and late origins of DNA replication. *Proc. Natl Acad. Sci. USA*, **96**, 9130–9135.